

Dynamics of re-constitution of the human nuclear proteome after cell division is regulated by NLS-adjacent phosphorylation

Gergely Róna^{1,2,*}, Máté Borsos^{1,3}, Jonathan J Ellis⁴, Ahmed M Mehdi^{5,6}, Mary Christie⁴, Zsuzsanna Környei⁷, Máté Neubrandt⁷, Judit Tóth¹, Zoltán Bozóky¹, László Buday¹, Emília Madarász⁷, Mikael Bodén^{4,8,9}, Bostjan Kobe^{4,8,10}, and Beáta G Vértessy^{1,2,*}

¹Institute of Enzymology; RCNS; Hungarian Academy of Sciences; Budapest, Hungary; ²Department of Applied Biotechnology and Food Sciences; Budapest University of Technology and Economics; Budapest, Hungary; ³Institute of Molecular Biotechnology of the Austrian Academy of Sciences (IMBA); Vienna, Austria; ⁴School of Chemistry and Molecular Biosciences; The University of Queensland; Brisbane, Queensland, Australia; ⁵Diamantina Institute; The University of Queensland; Translational Research Institute; Brisbane, Queensland, Australia; ⁶Department of Electrical Engineering; University of Engineering and Technology; Lahore, Punjab, Pakistan; ⁷Institute of Experimental Medicine of the Hungarian Academy of Sciences; Budapest, Hungary; ⁸Institute of Molecular Bioscience; The University of Queensland; Brisbane, Queensland, Australia; ⁹School of Information Technology and Electrical Engineering; The University of Queensland; Brisbane, Queensland, Australia; ¹⁰Australian Infectious Diseases Research Centre; The University of Queensland; Brisbane, Queensland, Australia

Keywords: cell cycle, dUTPase, importin, phosphorylation, trafficking

Abbreviations: dNTP, deoxyribonucleotide triphosphate; dTTP, deoxythymidine triphosphate; dUMP, deoxyuridine monophosphate; dUTP, deoxyuridine triphosphate; Cdc28, cyclin-dependent protein kinase (Cdk) encoded by CDC28; Cdk1, cyclin-dependent kinase 1; GO, gene ontology; NLS, nuclear localization signal; NES, nuclear export signal; cNLS, classical nuclear localization signal; SNP, single nucleotide polymorphisms; SV40, Simian virus 40; UBA1, Ubiquitin-activating enzyme E1; UNG2, Human Uracil-DNA glycosylase 2.

Phosphorylation by the cyclin-dependent kinase 1 (Cdk1) adjacent to nuclear localization signals (NLSs) is an important mechanism of regulation of nucleocytoplasmic transport. However, no systematic survey has yet been performed in human cells to analyze this regulatory process, and the corresponding cell-cycle dynamics have not yet been investigated. Here, we focused on the human proteome and found that numerous proteins, previously not identified in this context, are associated with Cdk1-dependent phosphorylation sites adjacent to their NLSs. Interestingly, these proteins are involved in key regulatory events of DNA repair, epigenetics, or RNA editing and splicing. This finding indicates that cell-cycle dependent events of genome editing and gene expression profiling may be controlled by nucleocytoplasmic trafficking. For in-depth investigations, we selected a number of these proteins and analyzed how point mutations, expected to modify the phosphorylation ability of the NLS segments, perturb nucleocytoplasmic localization. In each case, we found that mutations mimicking hyper-phosphorylation abolish nuclear import processes. To understand the mechanism underlying these phenomena, we performed a video microscopy-based kinetic analysis to obtain information on cell-cycle dynamics on a model protein, dUTPase. We show that the NLS-adjacent phosphorylation by Cdk1 of human dUTPase, an enzyme essential for genomic integrity, results in dynamic cell cycle-dependent distribution of the protein. Non-phosphorylatable mutants have drastically altered protein re-import characteristics into the nucleus during the G1 phase. Our results suggest a dynamic Cdk1-driven mechanism of regulation of the nuclear proteome composition during the cell cycle.

Introduction

Eukaryotic cells distribute proteins into various cellular compartments and these intracellular trafficking processes are under multiple levels of control. The transport of large macromolecules into and out of the nucleus depends on karyopherins, a group of proteins specifically recognizing short peptide segments in cargo proteins.¹ Peptide segments involved in these processes are termed nuclear localization signals and nuclear export signals (NLSs and NESs, respectively).² The recognition of NLS and

NES sequences by karyopherins can be effectively modulated by introducing negatively charged phosphate groups adjacent to the localization signals via protein phosphorylation. Such modifications have been shown to have a drastic effect on changing the cellular distribution of several proteins.^{3–5} The most extensive studies in this respect have been performed in yeast, while the human proteome has not yet been systematically investigated in this context.⁶

The best-characterized nuclear import pathway employs the transport factors importin- α (Imp α ; also known as karyopherin- α),

*Correspondence to: Gergely Róna; Email: rona.gergely@ttk.mta.hu; Beáta G Vértessy; Email: vertessy.beata@ttk.mta.hu

Submitted: 06/04/2014; Revised: 08/26/2014; Accepted: 08/28/2014

http://dx.doi.org/10.4161/15384101.2014.960740

and importin- β (Imp β). Imp α recognizes the cargo in the cytoplasm through binding to the classical nuclear localization signals (cNLSs), and the cargo enters the nucleus through nuclear pore complexes as a trimeric Imp α :Imp β :cargo complex. The directionality of transport through the nuclear pore complexes is determined by the small GTPase Ran, which has an asymmetric distribution of its nucleotide-bound states between the cytoplasm and the nucleus; it binds to Imp β inside the nucleus in its GTP-bound state, dissociating the import complex and releasing the cargo. Most cNLSs contain either one (monopartite) or 2 (separated by a linker sequence of usually 10–12 residues; bipartite) clusters of positively charged amino acids. Combining structural studies and interaction data for various cNLSs and their mutants has enabled the molecular understanding of the cNLS:Imp α recognition and the definition of cNLS consensus sequences. Imp α contains 2 cNLS-binding regions, the major and minor site. Bipartite cNLSs span both binding sites, while monopartite cNLSs usually bind preferentially to the major site. Individual amino acids in the cNLS bind to specific pockets in the cNLS-binding sites; in the bipartite cNLS consensus KRX_{10–12}KRRK (X corresponds to any amino acid),⁷ the N-terminal basic cluster corresponding to positions P1–P2' binds to the minor site, while the C-terminal cluster corresponding to positions P2–P5 binds to the major site.

Phosphorylation of proteins is mediated by protein kinases. The specificity of phosphorylation by a particular kinase depends on the composition of residues flanking the phosphorylation site (so-called peptide specificity),⁸ although it is further influenced by the context that the kinase finds itself in, including various forms of substrate recruitment.⁹ For example, the core consensus sequence for cyclin-dependent kinase 1 (Cdk1)-dependent phosphorylation sites has been described as [S/T*]-P-X-[K/R], where S/T* is the phosphorylated serine or threonine.^{10–12} More extensive analyses of known substrates and other available experimental data have uncovered further more subtle determinants of specificity for Cdk1 and other protein kinases.^{8,13,14}

Both NLSs and phosphorylation motifs can be described as linear motifs. Linear motifs are short sequences found most frequently in the disordered regions of proteins, and usually function in cellular signaling and regulation, by binding to protein interaction domains or by being the target of post-translational modifications.¹⁵ Although they pose difficulty for computational analysis because of their small size, significant progress has been made in the recent years in the computational identification of a number of different types of linear motifs and the integration of diverse types of experimental data into these computational approaches.¹⁵ In particular, we have developed some of the most reliable approaches for the identification of NLSs¹⁶ and protein phosphorylation sites.^{13,17} While computational predictions are often hampered by less than desired accuracies, combined prediction of 2 associated motifs can in fact lead to increased accuracy.¹⁸

The composition of the nuclear proteome defines the availability of the different proteins within the cell nucleus for dedicated functions. The role of cell-cycle dependent nucleocytoplasmic trafficking in regulatory processes of gene expression regulation, DNA damage and repair, and other genome editing

pathways have been partially investigated in yeast⁶ but have not yet been assessed systematically in mammalian cells. A fundamental difference between the 2 systems is the closed mitosis of yeast. During closed mitosis the nuclear membrane remains intact and the microtubule-based spindle extends within the nucleus.¹⁹ In case of open mitosis, cells temporarily lack their nuclear envelope in M phase. Thus, after mitosis the nuclear proteome has to be reconstituted from proteins that had passively diffused into the cytoplasm (except for the ones chromatin associated) and become excluded from the nucleus as the newly forming nuclear envelope is initially tightly attached to chromatin.²⁰ The modulation of the nuclear re-import of cargoes could give an additional layer of regulation of nuclear proteome composition throughout the cell cycle.

In the present study, we first carried out a computational analysis of the human proteome to identify putative regulatory Cdk1-dependent phosphorylation sites in the vicinity of NLSs in nuclear proteins. We then validated the computational predictions experimentally for a number of proteins, comparing the nucleocytoplasmic localization of hyper-phosphorylation mimicking (hyper-P; with a glutamic acid substitution) and non-phosphorylatable hypo-phosphorylation (hypo-P; with a glutamine substitution) mutants to the phosphorylatable wild-type (WT) protein in a new cellular assay. Finally, we selected one particular protein as an in-depth case study to analyze the dynamics of phosphorylation-regulated nuclear transport during the cell-cycle. We selected human dUTPase, a protein involved in genomic integrity,²¹ for this case study; where we have previously characterized the molecular and structural basis of NLS-adjacent phosphorylation on nuclear import.²² Namely, the introduction of negative charge into the P-1 position rearranges the accommodation pattern of the dUTPase NLS in the importin- α NLS binding site. This results in the loss of critical hydrogen bonds between the importin- α surface and the NLS peptide, impairing nuclear import.²² Here, we show that Cdk1-dependent phosphorylation of dUTPase results in a scheduled, dynamic pattern of nuclear availability in the newly-formed daughter cells. Jointly, our results uncover a ubiquitous mechanism for the regulation of nuclear trafficking of human proteins by Cdk1 during the cell cycle and provide a molecular explanation for the negative regulation of nuclear import by NLS-adjacent Cdk1-dependent phosphorylation.

Results/Discussion

The effect of NLS-adjacent phosphorylation on nucleocytoplasmic protein distribution during the cell cycle

Earlier publications identified several yeast⁶ and human proteins,^{3,4,22} where NLS-adjacent phosphorylation was shown to inhibit nuclear import. In these cases, phosphorylation took place at either the P0 or the P-1 positions of the NLS, immediately N-terminal to the large basic cluster of the NLS.²³ Yeast Cdc28 or its human orthologue Cdk1, were proposed to be responsible for most of these phosphorylation events, thus giving these proteins a cell cycle-specific localization pattern.⁶ Cdc28 and Cdk1 phosphorylate a number of proteins that control critical cell cycle

Table 1. Proteins covering different functions within the cell selected for further analysis from the proteome-wide screen. Proteins for which the phosphorylation of the particular NLS adjacent residues were experimentally confirmed, according to the Phosida database (<http://www.phosida.com/>)^{62,63} are indicated in italics

Function	Protein name	Abbreviation	NLS sequence	Ref.
DNA damage recognition and repair	<i>Ataxia telangiectasia and Rad3-related protein</i>	ATR	SPKRRRLS	64
	BRCA1-A complex subunit RAP80	UIMC1	SVKRRKRL	65,66
	Cullin-4B	CUL4B	TSAKKRKL	67
	<i>Transcription factor AP-4</i>	TFAP4	SPKRRRAE	68
	Histone acetyltransferase p300	EP300	SAKRPKLS	69
	Ras-responsive element-binding protein 1	RREB1	SPLKRRRL	70
Regulation of gene expression	Ras-responsive element-binding protein 1	RREB1	SPLKRRRL	71
	Histone acetyltransferase p300	EP300	SAKRPKLS	72
	Transcription factor AP-4	TFAP4	SPKRRRAE	68,73,74
Epigenetics	Histone acetyltransferase p300	EP300	SAKRPKLS	69
	Bromodomain adjacent to zinc finger domain protein 2A	BAZ2A	SPSKRRRL	75,76
	Cullin-4B	CUL4B	TSAKKRKL	77
RNA editing/splicing	Ser-Arg repetitive matrix protein 2	SRRM2	TPAKRKRR	78
	Cyclin-L2	CCNL2	SPKRRKSD	79
Cell cycle regulation	Cullin-4B	CUL4B	TSAKKRKL	80-82
	Cyclin-L2	CCNL2	SPKRRKSD	79,83
Development	T-cell leukemia homeobox protein 3	TLX3	TPPKRKKP	84
	<i>Transcription factor AP-4</i>	TFAP4	SPKRRRAE	68
Nuclear skeleton	<i>Lamin A</i>	LMNA	SVTKKRKL	85,86

events, including DNA replication and segregation, transcriptional programs and cell morphogenesis.²⁴ The available results clearly argue for the importance of Cdk1-kinase-regulated nuclear transport for several yeast proteins involved in the regulation of cell cycle progression, DNA replication, DNA damage recognition and repair. As we presently show, similar regulation may occur for human proteins of similar function (Table 1).

We set out to perform a human proteome-wide bioinformatics screen with the aim of identifying human proteins possessing a Cdk1-dependent phosphorylation site at either P0 or P-1 positions of their NLS. We combined 2 state-of-the-art bioinformatics tools for prediction of NLSs (NucImport¹⁶) and phosphorylation sites (Predikin¹³) that we ourselves developed previously. NucImport uses a probabilistic (Bayesian network) approach to recognize a variety of NLSs by integrating amino acid sequence and interaction data and predicts the sequence position of the NLS, outperforming other available methods.¹⁶ Predikin uses the concept of specificity-determining residues to predict peptide specificity of protein kinases and identify substrates for protein kinases^{14,17,25}; the tool outperformed other competing tools in the protein kinase section of the Peptide Recognition Domain specificity prediction category of the 2009 DREAM4 challenge (an independent test using unpublished data).¹³ We first used Predikin¹³ to determine how often a Ser or Thr residue was predicted to be phosphorylated, regardless of the import status or presence of NLS. This background frequency of phosphorylation was determined to be 0.136 (c.f. Experimental Procedures). We then used NucImport¹⁶ to predict the location of classical NLSs. For each NLS location, we determined the frequency of (predicted) phosphorylation of the P0 position to be 0.393 ($p = 2.348e-30$) and of the P-1 position to be 0.234 ($p = 9.530e-05$). Hence, both positions are significantly enriched for phosphorylation.

Overall, with a conservative setting of both predictors (see Experimental Procedures for details), we found 92 proteins with a

phosphorylation site in the P0 position and 44 proteins with a phosphorylation site in the P-1 position, considering all protein isoforms (if considering only parent proteins, this corresponds to 50 and 22, respectively; Table S1). Among these proteins, there are numerous examples for which, to our knowledge, no previous experimental data have been reported as being relevant to phosphorylation-dependent nuclear translocation. Using Gene Ontology (GO) term annotations, we found proteins involved in DNA damage recognition and repair, gene expression, epigenetics, RNA-editing and several transcription factors (Table 1; Table S2). For any of these functions, strict and regulated scheduling of nuclear availability has clear and imminent significance, arguing for the need for further direct experimental study. We therefore selected several identified proteins for experimental validation.

Cellular screen to evaluate NLS function for selected proteins

To efficiently test the effect of phosphorylation on nuclear import for a number of proteins, we designed a sensitive model system. We chose DsRed-monomer labeled β -galactosidase, a well-described bacterial protein, as an inert fluorescent cargo, upon which different NLSs can be loaded. The construct is strictly cytoplasmic, unless fused to a functional NLS, such as the well-established SV40 large T-antigen (TAg) NLS (Fig. 1A). In order to evaluate phenotypic characteristics of any further NLSs, we set a measure scale for 5 distinct cellular distribution patterns (Fig. 1B). We tested this NLS reporter system using the WT and mutant NLSs of the Swi6 protein (Fig. 2A), which has been previously described to be phosphorylated at the P-1 position of its NLS by Cdc28, resulting in the inhibition of its nuclear transport.^{6,26-28} The mutations were introduced in such a way that the negative charge, mimicking the phosphorylated residue, was introduced either at the P-2, P-1 or P0 positions,²³ while the

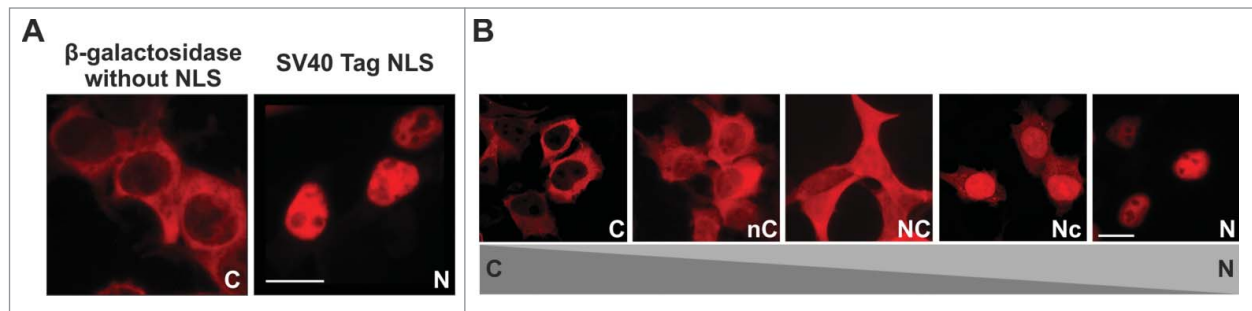


Figure 1. Representation of relative NLS activity. (A) The β -galactosidase-DsRed (pGal-DsRed) reporter construct is strictly cytoplasmic, unless fused to a functional NLS, such as the SV40 large T-antigen (TA) NLS. Scale bar represents 20 μ m. (B) The reporter construct was fused with various NLSs to generate constructs with different extents of nuclear localization. Localization was categorized into 5 types: N (completely nuclear), Nc (mainly nuclear), NC (homogenous distribution between the nucleus and cytoplasm), nC (mainly cytoplasmic), C (completely cytoplasmic). Scale bar represents 20 μ m.

structurally important proline residue was not perturbed (Fig. 2B).

The results argue that the exact position of the phosphorylated residue is a crucial determining factor in the localization of NLS-containing cargo. Our results are in good agreement with previous work proposing that phosphorylation at P0 or P-1 positions impedes nuclear import, while on the other hand, phosphorylation at upstream positions, for example in the P-2 position, have the opposite effect by enhancing nuclear import.²⁹

Using the validated screening system, we tested a selection of proteins involved in a variety of cellular functions (Table 1 and references therein). Our selections included 6 proteins with

predicted Cdk1 phosphorylation sites at the P0 position, and 7 proteins with predicted Cdk1 phosphorylation sites at the P-1 position (Table S3). The resulting localization data in Figure 3 show that in each case, substitution of the appropriate Ser or Thr, predicted to be phosphorylated by Cdk1, by Glu (hyper-P mimicking) consistently leads to significantly weaker nuclear accumulation or even to complete nuclear exclusion, compared to the WT protein. The efficiency of nuclear targeting differed among the different NLSs. Our experimental data further argue for the inhibitory effect of the phosphorylation at the P-1 and P0 positions on nuclear import, and confirms the validity of the in silico analysis. Among the hits of the in silico screening dUTPase

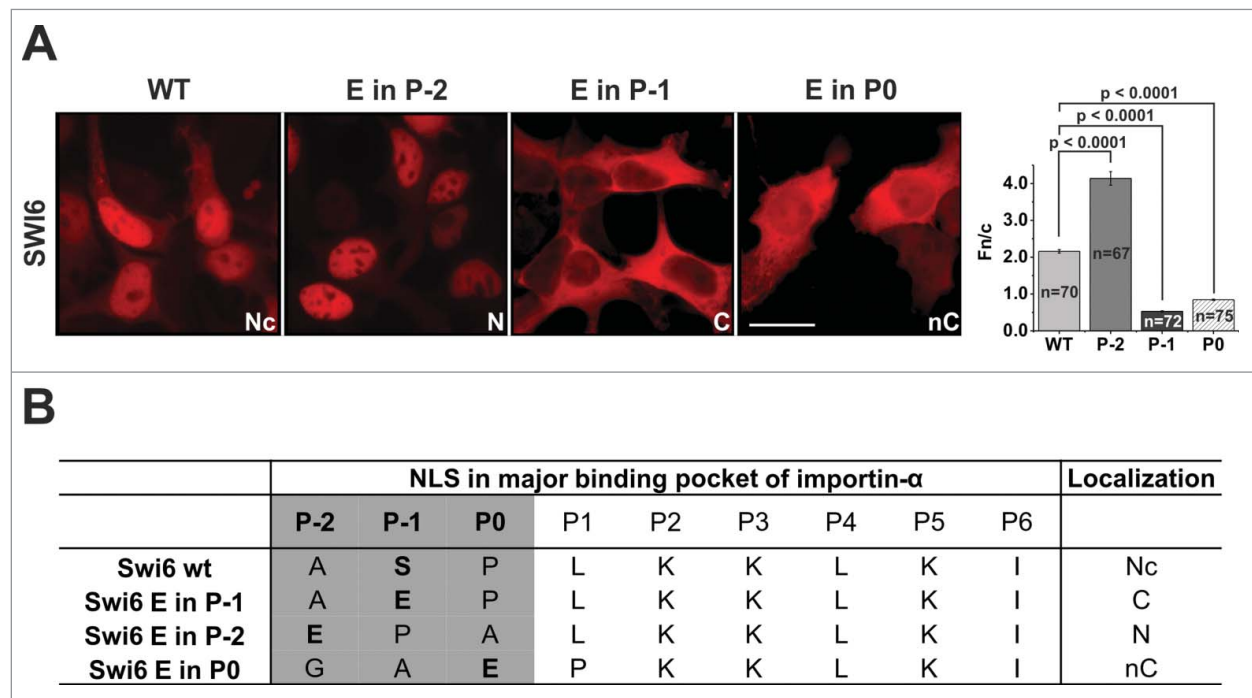


Figure 2. Position-specific effect of phosphorylation on NLSs. (A) Performance of the reporter system (pGal-DsRed) after fusing Swi6 WT and mutant NLSs to the construct. $F_{n/c}$ ratios (\pm standard error of the mean) were determined as described in the Experimental Procedures section. Localization pattern was categorized according to Figure 1B. Scale bar represents 20 μ m. (B) Glutamic acid at P-2 or P0 was introduced by insertion of Ala in P0 or deletion of Leu in P1. Sequences were aligned as predicted to bind to the NLS-binding pockets of importin- α .²³

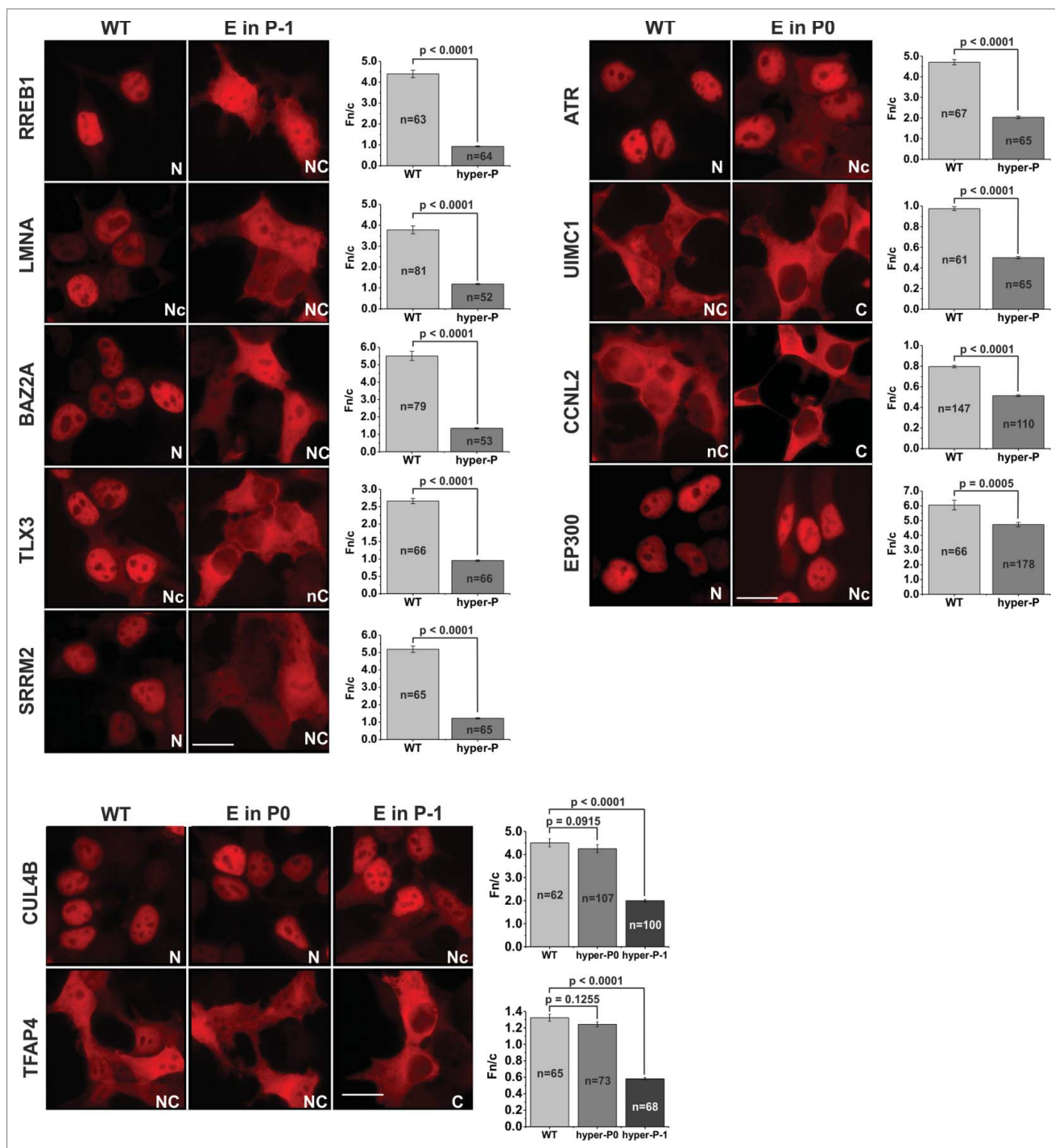


Figure 3. Evaluation of the proteins identified by computational analysis: cellular screens for NLS activity. Localization patterns of selected proteins selected based on proteome-wide analysis. DNA corresponding to NLSs was cloned into the pGal-DsRed reporter system, and localization was tested in 293T cells. P-mimicking mutations at the appropriate Ser/Thr position in most cases significantly reduced nuclear accumulation. Scale bar represents 20 μ m.

was not present due to the strict settings of NuImport. However its NLS was tested in our reporter system, which showed nuclear exclusion upon Glu substitution in the P-1 position in agreement with our previous data on full length protein (Fig. S1A).²² Our analysis thus identified numerous

human proteins potentially sharing a similar Cdk1-driven regulatory pattern (Table 1; Table S1). These proteins are involved in crucial cellular functions such as DNA damage recognition and repair, transcriptional regulation, cell cycle control, epigenetics and RNA editing.

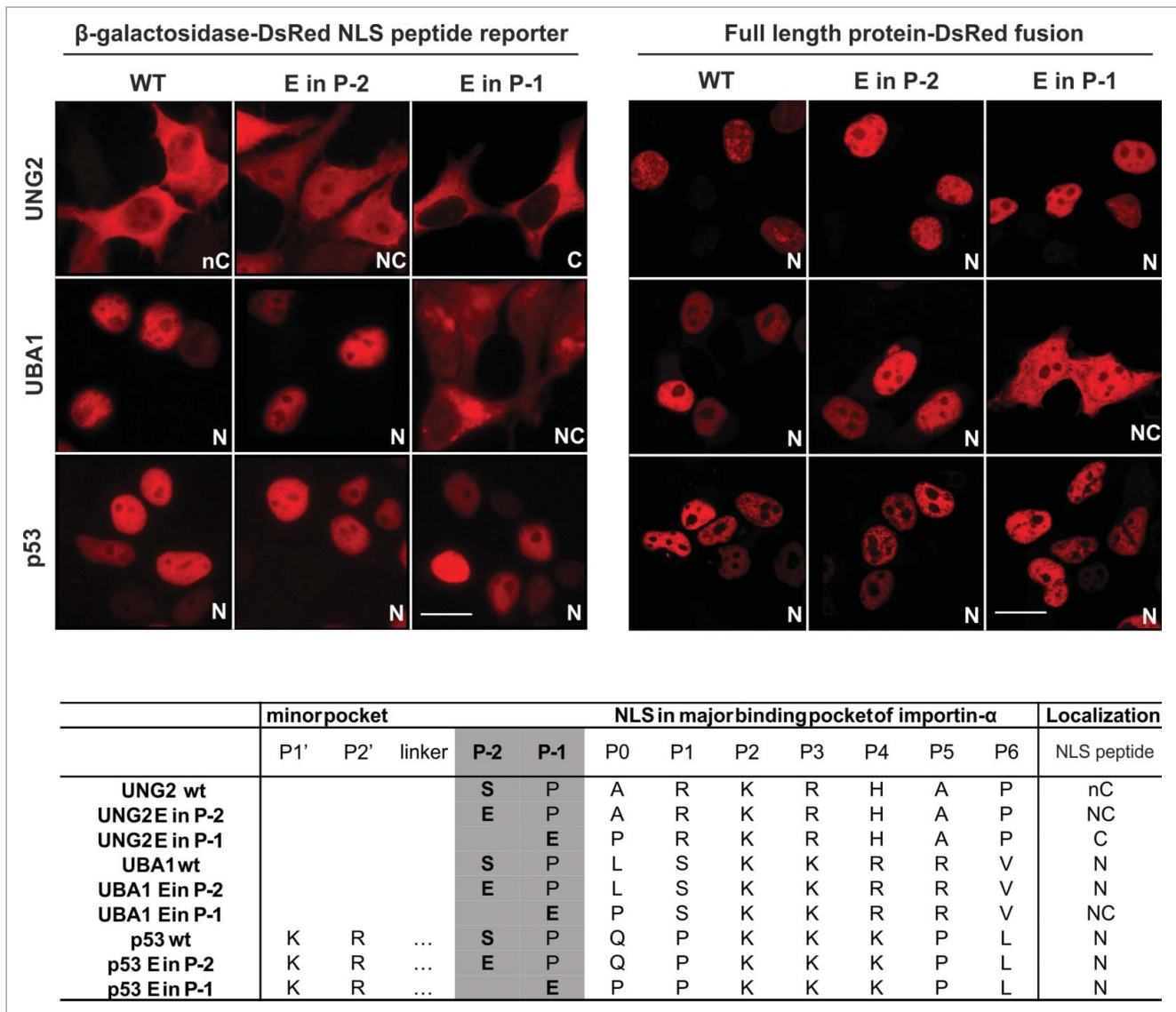


Figure 4. Effect of phosphorylation on localization of Cdk1 substrate proteins. UNG2 (residue S14), UBA1 (residue S4) and p53 (residue S315) phosphorylation at the P-2 positions of their NLSs were mimicked by Glu substitution in the pGal-DsRed reporter system or were mutated in full length proteins fused to DsRed-monomer. Localization was tested in 293T cells. Scale bar represents 20 μ m.

For several proteins where NLS-adjacent Cdk1-driven phosphorylation has been reported previously, its actual effects could not be properly deciphered when using only hypo-P mimicking mutants in static or kinetic experiments. Therefore, we checked the effect of hyper-P mimicking mutations at the previously established Cdk1 sites of UNG2 (S14 phosphorylation^{30,31}), UBA1 (S4 phosphorylation³²) and p53 (S315 and S312 phosphorylation in human and in mouse, respectively³³) (Fig. 4). The NLS segments were cloned into our pGal-DsRed NLS reporter construct and the full length ORFs were fused with DsRed-monomer for localization studies. These phosphorylation sites are predicted to be located in the P-2 position adjacent to their NLSs. As expected, a negative charge introduced at this

position did not abolish the nuclear localization of either of these constructs (both with the NLS reporter and the full length proteins). However, if we used mutagenesis to move this negative charge to the P-1 position, the impeding effect on nuclear import is clearly observable in case of UBA1 and UNG2 (Fig. 4) with the NLS reporter constructs. In case of the UNG2 it is clearly visible that the nuclear localization is enhanced in the S14E mutant (in P-2 position), and the nuclear targeting capability of the WT NLS is evident when compared to the NLS impaired mutant, K18N (Fig. S1B and C).³⁴ Phosphorylation of the P-2 positions might enhance nuclear accumulation of these proteins after mitosis. Possible reason why the full length UNG2 does not show the same localization pattern as the NLS reporter construct is that it

has a complex NLS which not exclusively relies on the S¹⁴PARKRHA sequence. Perturbation of this segment does not lead to complete nuclear exclusion, other sequences also have a role in proper localization of UNG2.³⁴ p53, which harbors a bipartite NLS sequence, might have the flexibility to compensate these negative effects by the additional binding to the minor NLS-binding site.

Video microscopy-based kinetic analyses

To have a better understanding of the effect of the described phosphorylation on the dynamic distribution of proteins throughout the cell cycle, we used dUTPase as a model. This enzyme catalyzes the hydrolysis of dUTP into dUMP and inorganic pyrophosphate³⁵⁻³⁷ preventing dUMP incorporation into DNA.^{38,39} dUTPase is an important contributor to genomic integrity from bacteria to human^{21,40-45} and possesses a nuclear

isoform in different eukaryotes.^{40,46,47} We have previously shown that the cell cycle-dependent phosphorylation of dUTPase by Cdk1 at the S11 position (which is located in the P-1 position of its NLS^{46,48}) abolishes its nuclear import and is linked to M phase.²²

In order to follow the dynamic alterations of dUTPase localization pattern during the cell cycle, we followed individual cells after transfection with the appropriate fluorescent constructs by video microscopy. The dUTPase pool exhibits marked cell cycle-dependent dynamic behavior (Fig. 5A). When the new nuclear envelope appears, dUTPase is excluded from the nucleus. Following cytokinesis, it takes a considerable time before the nuclear space is again re-populated with WT dUTPase (Video S1 left panel). Interestingly, for the S11Q mutant, the nuclear repopulation dynamics is markedly different (Video S1 right panel). The S11E mutant, by contrast, remains cytoplasmic during the entire cell cycle (Video S2).

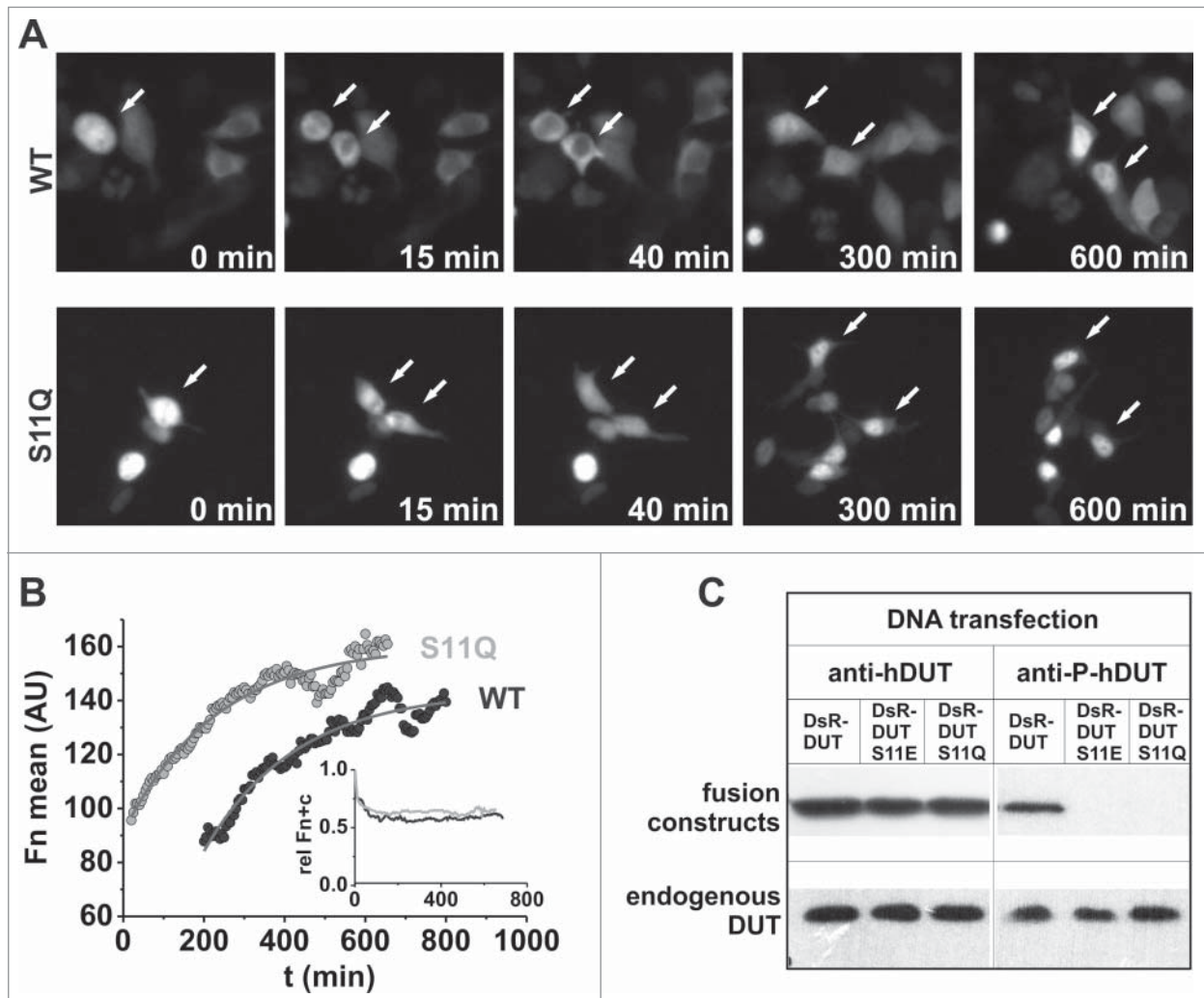


Figure 5. Phosphorylation-dependent cellular localization pattern of dUTPase. **(A)** Live-cell microscopy of daughter cells. Transfected 293T cells were observed during at least one full cell cycle. Still images were taken from Video S1. The once-nuclear pool gets slowly re-imported into the nucleus. **(B)** Kinetic analysis of protein re-import dynamics of the daughter cells indicate similar import kinetics but different lag phases for the WT protein and the S11Q mutant ($k_{obs} = 0.0044 \text{ min}^{-1} \pm 7\%$ and $0.0043 \text{ min}^{-1} \pm 8\%$, respectively). **(C)** Western blot shows cognate phosphorylation of exogenous dUTPases.

Using this approach, we could measure apparent rate constants for nuclear re-accumulation of the WT and the S11Q mutant dUTPases (Fig. 5B). The same approach cannot be applied to the S11E mutant, as it never enters the nucleus in our experiments. We found that the major difference between the WT protein and the S11Q mutant is that the WT protein re-enters the nucleus with a considerable lag. Following the lag phase, the apparent rate constants of nuclear accumulation are identical for the WT protein ($k_{\text{obs}} = 0.0044 \text{ min}^{-1} \pm 7\%$) and for the S11Q mutant ($k_{\text{obs}} = 0.0043 \text{ min}^{-1} \pm 8\%$). Importantly, the mean total fluorescence of the cells ($F_{\text{n+c}}$) did not change during our observations (Fig. 5B inset), indicating the steady-state of the investigated fluorescent protein pool. The apparent single exponential kinetics we observe likely represents the result of multiple undistinguishable transport events. The fact that the wild type protein and the non-phosphorylatable mutant S11Q show different kinetic behavior is clearly due to the change in their phosphorylatable properties.

In order to directly address the pattern of nucleocytoplasmic trafficking of a given protein pool, we repeated the video-microscopy experiments by transfecting the fluorescent proteins themselves, instead of plasmids that lead to continuous expression. Cells transfected with recombinantly expressed WT and S11Q DsR-DUT proteins show the same dynamic events of dUTPase pool distribution as those in the plasmid transfection experiments (Figure S2 and Videos S3 and S4).

To investigate whether the exogenous DsR-DUT constructs (originating either from transfected plasmids or the recombinant protein itself) used in the video-microscopy experiments can be phosphorylated similarly to the endogenous protein, we performed western blot experiments (Fig. 5C; Fig. S3B). We used a dUTPase-specific antibody generated against the full-

length protein (anti-hDUT⁴³), in combination with the dUTPase S11-phosphoserine specific antibody (anti-S11P-hDUT²²). Figure 5C shows that 293T cells transfected with the appropriate fusion protein-encoding plasmids produce a WT DsR-DUT protein pool that can be phosphorylated. The recognition of dUTPase by the anti-S11P-hDUT antibody is observed only if Ser11 can be phosphorylated, providing evidence for the specificity of this antibody. The endogenous dUTPase pool is also visible at a lower molecular mass position. Neither forms of recombinant proteins produced in *E. coli* are recognized by the anti-S11P-hDUT antibody, indicating that they are not phosphorylated at Ser11 (Fig. S3B). Within the cells transfected with recombinantly produced DsR-DUT protein itself, however, the cognate phosphorylation event targeting Ser11 can take place. The anti-hDUT antibody recognizes all dUTPase construct forms, as well as the endogenous dUTPase pool, independently of the point mutation or phosphorylation state (Fig. S3B).

The P-mimicking mutation leads to the exclusion from the nucleus, resulting in an interesting observation that the nuclei of the daughter cells become populated with dUTPase protein only after a significant delay. These results indicate that the potential of the WT protein to be phosphorylated within the nucleus may have physiological implications manifested in its retarded re-import in the daughter cells. The non-phosphorylatable S11Q construct does not exhibit this behavior. We suggest that this mechanism may also operate for the proteins listed in Table S1, because they contain similar phosphorylatable NLSs. Assuming similar nuclear re-import characteristics as that of dUTPase, Cdk1 kinase-induced phosphorylation at these NLS positions would significantly alter the nuclear proteome re-establishment in the daughter cells after the M phase (Fig. 6).

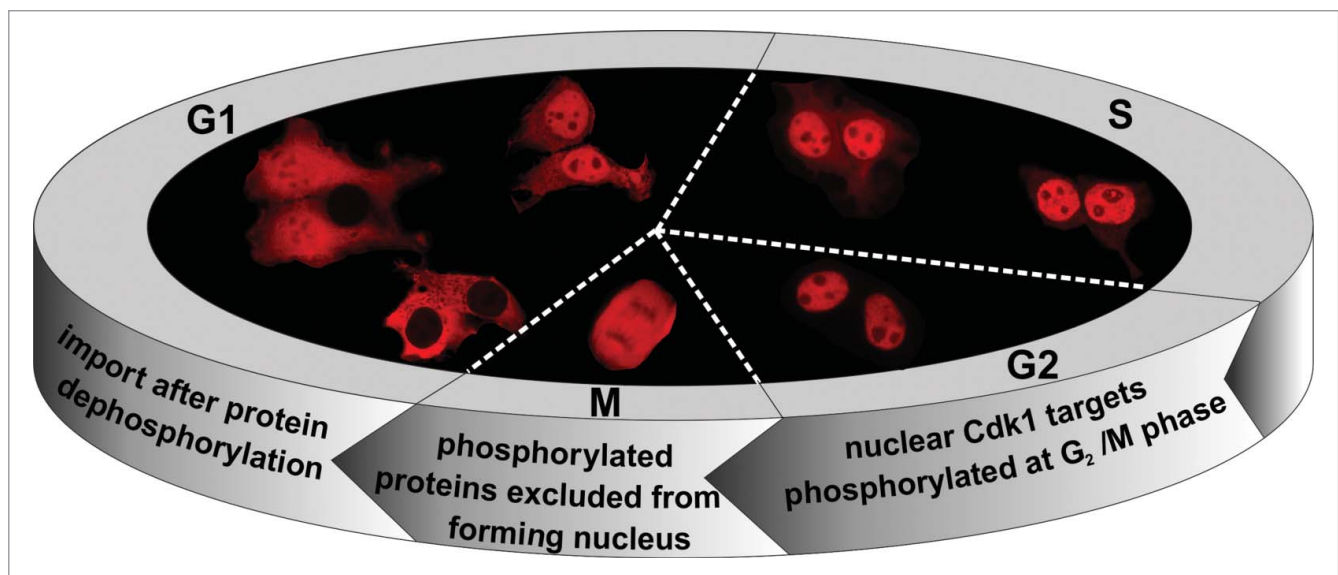


Figure 6. Reconstitution of the nuclear proteome after cell division. Schematic diagram of the model of nuclear proteome re-setting through regulation of nuclear import by Cdk1 phosphorylation during the cell cycle in human cells.

Biological significance of cell-cycle dependent re-shaping of the nuclear proteome

Our studies suggested that Cdk1 kinase-induced phosphorylation of many human proteins potentially alter their localization patterns during the cell cycle. Specifically, the most detailed kinetic analysis performed in our case study using dUTPase indicated that the re-import into the nucleus is delayed significantly if the relevant site close to the NLS segment is phosphorylated. Although the mechanism by which this cell-cycle-dependent localization pattern is governed seems to be general (cf Fig. 6), the exact physiological consequences of these effects depend on the actual protein and its role in cellular pathways. Below, we discuss these protein-specific characteristics.

In the case of dUTPase, Cdk1-induced phosphorylation of the protein within the nucleus at the G2/M phase will have a prominent effect on the dUTPase pool localization in daughter cells. Namely, dUTPase nuclear import is hampered until the phosphate moiety is removed, thus nuclear re-population in the daughter cells takes place only after a considerable time delay. dUTPase nuclear accumulation reaches its maximal extent around the S phase and the protein remains strictly nuclear until the onset of mitosis (Fig. 5A). Recently, it has been shown that nuclear localization of the de novo thymidylate biosynthesis pathway is required for the maintenance of genomic integrity.⁴⁹ This is achieved by sumoylation-mediated nuclear transport of the enzymes of the pathway, composed of thymidylate synthase (TYMS), dihydrofolate reductase (DHFR), and serine hydroxymethyltransferase (SHMT1 and SHMT2 α).^{50,51} For all these enzymes, this partial nuclear translocation takes place at the onset of S phase, and they remain in the nucleus until the G2/M phases, while they are cytoplasmic during G1 phase, enabling de novo thymidylate synthesis during DNA replication and repair.⁵² dUTPase catalyzes the hydrolysis of dUTP into pyrophosphate and dUMP; ensuring the substrate for TYMS, and also low cellular dUTP/dTTP ratios, thus inhibiting uracil accumulation in the DNA.²¹ Here we show that dUTPase nuclear accumulation also reaches its maximal extent during the S phase, similarly to the de novo thymidylate biosynthesis enzymes. Because it was suggested that de novo thymidylate biosynthesis does not occur in the cytoplasm at rates sufficient to prevent uracil misincorporation into DNA,⁴⁹ it is reasonable to propose that dUTPase might also be necessary to accompany this enzyme complex into the nucleus for proper genomic DNA maintenance. Partially due to S phase activation of ribonucleotide reductase subunits, regulated by transcriptional and post-transcriptional processes, the dNTP pool in mammalian cells increases 20-fold at this cell cycle stage compared to G1.⁵³ Thus scheduled nuclear availability of de novo thymidylate biosynthesis enzymes, along with dUTPase and ribonucleotide reductase, may ensure strictly regulated dNTP pool composition for DNA polymerases.

Table 1 provides a list of other human proteins where we found potential Cdk1 sites and suggest that phosphorylation regulates their nuclear import and thus their availability in the nucleus. These proteins are involved in crucial cellular functions such as DNA damage recognition and repair, transcriptional regulation, cell cycle control, epigenetics and RNA editing. Clearly,

for proteins involved in such functions, the fine-tuned regulation of nuclear availability is of high significance. For example, cullin-4B plays a role in cell cycle regulation together with cyclin-L2, which is also involved in pre-mRNA splicing, alongside with apoptosis induction and cell-cycle arrest in cancer cells. The ataxia telangiectasia and Rad3-related protein, BRCA1-A complex subunit RAP80 and histone acetyltransferase p300 are key components of DNA damage repair. We also found that many of these proteins may act in an interconnected manner; for example, during DNA damage, the protein kinase ATR phosphorylates the bromodomain adjacent to Zn-finger domain protein 2a, the BRCA1-A complex subunit RAP80, the Ras-responsive element binding protein 1, and the Ser/Arg repetitive matrix protein 2.⁵⁴ For proteins involved in DNA repair (ATR, cullin 4B, BRCA1-A subunit RAP80, transcription factor AP-4), the tight connection between cell-cycle checkpoints and DNA damage recognition and response pathways may be the underlying reason for their scheduled absence or presence within the nucleus.⁵⁵ Such regulation of protein subcellular distribution may assist in maintaining the correct logistics of scheduling and executing different tasks during the cell cycle along with the regulation of mRNA nucleocytoplasmic trafficking.⁵⁶ In such a way, the use of crucial metabolites involved in energy and signal transduction can also be correctly distributed among cell division, replication and repair tasks. Interestingly, examination of SNP databases revealed 2 instances where a given SNP may overwrite the Cdk1 driven regulation, however, no data for either frequency or physiological relevance of these SNPs has been reported (Table S1).

Conclusions

Dynamic exchange of macromolecules between the cytoplasm and the nucleus is regulated by several mechanisms. Here we suggest that nuclear import is significantly delayed for those cellular proteins where a Cdk1 kinase-dependent phosphorylation event occurs during the M phase at a relevant site in the vicinity of the NLS (Fig. 6).

Two bioinformatics tools, namely NuclImport and Predikin, were used to identify the scope of the hypothesized mechanism and to isolate candidate targets. We established the statistical basis for identifying relevant hits and their functional (gene ontology) associations, in ways not supported by the tools individually. Albeit not implemented as a tool in its own right, our integrated approach, may help to develop further studies that aim to understand how (other) post-translational modifications can dynamically modulate functions of sequence motifs (including localization signals). Our analysis showed that (i) positions P-1 and P0 relative to predicted human NLSs are both significantly enriched for predicted Cdk1 phosphorylation; and (ii) 44 and 92 protein isoforms (with phosphorylation of NLS P-1 and P0 sites, respectively) are associated with a range of functions that require strict and regulated scheduling of nuclear availability.

Our cellular reporter assay confirmed the computational predictions of proteins regulated by NLS-adjacent phosphorylation

and showed that Cdk1 phosphorylation at P-1 and P0 positions of human NLSs impedes nuclear import. Although the observed effects may be modulated in the full-length proteins, our results clearly provide proof-of-concept. Namely, we propose that the cell cycle-dependent changes in the nuclear proteome may have an important role in selecting the correct set of proteins to be present in the nucleus during the different stages of the cell cycle. Cdk1 phosphorylation events at the M phase will result in proteins that cannot be re-imported into the nucleus after cytokinesis, because phosphorylation of the P-1 and P0 positions impedes their binding to importin- α . Therefore, several proteins will only appear in the nucleus of the daughter cells after a significant delay following dephosphorylation or de novo protein synthesis. Dephosphorylation in the cytoplasm may require some time and might be under yet another level of regulation, giving cells further plasticity in fine-tuning their nuclear proteome. The regulatory pattern we described may prevent accumulation of proteins within the nucleus that could perturb cellular functions, for example by initiating expression of genes with an incorrect schedule. This regulation might also be further fine-tuned by cytoplasmic anchoring processes, facilitated by phosphorylation events.⁵⁷ However, the exact purpose of this regulation might differ for each protein, and should be checked individually in detail.

Cell cycle-dependent changes in the nuclear proteome are of utmost importance in the prompt regulation of cellular events, and protein kinases such as Cdk1 cooperate to control the cell cycle dynamics. After cell mitosis, daughter cells form their own nuclear envelope and begin with a limited set of proteins that remain strictly adherent to the chromosomes during cytokinesis.²⁰ Organism, like yeast, with closed mitosis rely on active protein transport in every phase of their cell-cycle while cells with open mitosis thus have the unique opportunity of re-setting the protein composition within the nucleus of daughter cells after every division. We conclude that Cdk1-driven phosphorylation at P-1 or P0 positions of the NLSs makes a significant contribution to this re-shaping process of the nuclear proteome after the M phase.

Materials and Methods

Computational analyses of NLSs and phosphorylation motifs

The computational tools Predikin¹³ and NuclImport¹⁶ were used to analyze the human proteome. Protein sequences were obtained from UniProt⁵⁸ as the complete human proteome including all known isoforms, as defined by UniProt complete proteome sets (representing a total of 71,809 sequences).

To predict the location of nuclear localization signals, we used NuclImport.¹⁶ NuclImport predicts the probability of nuclear import, type of classical NLS (as categorized by⁵⁹) and its exact location in any query protein sequence. Apart from sequence properties, the prediction is based on known (human) protein interactions that are retrieved from BioGRID.⁶⁰ We refer to the predicted proteome set as those proteins that were assigned a type-1 classical NLS with a probability of 0.95 or greater.

Cdk1 phosphorylation sites were predicted for all potential sites, i.e., all Ser and Thr residues, using Predikin.¹³ As we used the Cdk1 matrix to score all potential phosphorylation sites in the human proteome, we obtained the complete distribution of scores associated with Cdk1. Converting these to a cumulative density allowed us to (empirically) determine p-values associated with each Predikin score (the p-value is the probability of achieving a score at least as high as the one observed).

We looked for enrichment of phosphorylation at the P0 and P-1 sites relative to the (predicted) NLS in each protein in the nuclear proteome by counting, for each NLS site, all potential phosphorylation sites (i.e., all Ser and Thr sites) that do not occur at the NLS site of interest and recorded whether they are above or below a threshold (Predikin p-value = 0.1). From these counts, the ratio of phosphorylation sites/potential sites can be calculated for the background, P0 and P-1 positions. We assessed whether observations at P0 and P-1 differed from the background by performing a χ^2 analysis.

Gene Ontology (GO) term enrichment analysis was performed for identified proteins using Fisher's exact test. Specifically, we used all proteins predicted to have a type-1 classical NLS and a predicted phosphorylation site at either P0 or P-1 as a foreground, and all "reviewed" human proteins in UniProtKB as background. We used the Gene Ontology official release of human annotations (as of February 2012). For each biological process GO term, we counted the number of proteins in the foreground set and the background set with this term. The one-tailed Fisher's exact test establishes the p-value of the term: the probability of finding this protein count or more extreme (greater proportion in the foreground). The p-value was corrected for multiple testing (shown as E-value). A term is thus assigned a small E-value only if proteins annotated with that term occur in the foreground set with a higher prevalence than can be statistically explained by chance (i.e. proteins picked randomly from the background set).

Cell culture and constructs

293T cells were kindly provided by Prof. Yvonne Jones (Cancer Research UK, Oxford). Cells were cultured in DMEM/F12 HAM (Sigma) supplemented with Penicillin–Streptomycin solution (50 μ g/ml; Gibco) and 10% FBS (Gibco). dUTPase nuclear isoform (DUT) fused to DsRed-Monomer (DsR-DUT) was described in.²² DsR-DUT was further cloned into the NdeI/XhoI sites of the vector pET-20b (Novagen) for recombinant protein expression (with oligonucleotides dutpETF and dutpETR). Human tumor protein p53 cDNA was purchased from OriGene (NM_000546.2). p53 was fused to DsRed-Monomer, by cloning it into the XhoI/BamHI sites of a modified pEGFP-C1 vector (Clontech) (with primers p53_F and p53_R), where EGFP was replaced by DsRed-Monomer (within the NheI/XhoI sites of the vector). Ubiquitin-activating enzyme E1 (UBA1) cDNA was purchased from OriGene (NM_003334.2) and the fusion construct was made cloning it into the KpnI/BamHI sites of the pDsRed-Monomer-N1 vector (Clontech) (with primers UBA1_F and UBA1_R). Human Uracil-DNA glycosylase 2 (UNG2) cDNA was a generous gift of Professor Salvatore

Caradonna and was cloned into the XhoI/KpnI sites of the pDsRed-Monomer-N1 vector (with primers UNG2_F and UNG2_R). Site-directed mutagenesis was performed by the QuickChange method (Stratagene). The NLS reporter construct was created by fusing β -galactosidase with DsRed-Monomer (termed pGal-DsRed). β -galactosidase was amplified lacking its start codon from the vector pCAUG (with oligos galN1F and galN1R), and was cloned into the KpnI/EcoRI sites of the vector pDsRed-M-N1, thus generating the vector termed pGal-DsRed. Single-stranded oligonucleotide pairs, listed in Table S4, encoding different NLS peptides were cloned into the NheI/EcoRI sites of the pGal-DsRed vector after annealing. In addition, the vector pHM830 (Addgene plasmid 20702) (AflII/XbaI sites) was also used to generate constructs for the NLSs that showed a strong tendency for aggregation when used in context of the previously described pGal-DsRed construct.⁶¹ Primers used for cloning and mutagenesis were synthesized by Eurofins MWG GmbH and are summarized in Table S4. All constructs were verified by sequencing at Eurofins MWG GmbH.

Fluorescence imaging and analysis of DsRed-tagged constructs

For DNA transfections, LipofectamineTM LTX (Invitrogen) was used according to the manufacturer's instruction. Briefly, subconfluent cultures of 293T cells grown in 35 mm Petri dishes were incubated with 1-2 μ g DNA along with 10 μ l LTX reagent in serum-free medium, for 16 hours. Protein transfection was performed according to the manufacturer's protocol using Pro-DeliverINTM reagent (OZ Biosciences). In brief, 8-10 μ g protein and 15 μ l transfection reagent was used to deliver DsRed-tagged proteins into the cells for 14-18 hours. Image analysis to quantify relative subcellular localization was performed from single-cell measurements using ImageJ 1.46j (NIH, Bethesda), where the mean nuclear (F_n) and cytoplasmic (F_c) fluorescence ratio ($F_{n/c}$) was measured within each cell. Statistical analysis of the relative subcellular localization changes was carried out by the InStat 3.05 software (GraphPad Software, San Diego California, USA) using the non-parametric Mann-Whitney test. Differences were considered statistically significant at $P < 0.05$. Images were either acquired with a Leica DM IL LED Fluo microscope equipped with a Leica DFC345 FX monochrome camera.

Live-cell microscopy and evaluation

Time-lapse recordings were performed on a Zeiss 200 M inverted microscope equipped with an AxioCam Mnr camera and controlled by the AxioVision 4.8 software. Cells were cultured in Ibidi dishes and kept at 37°C in a humidified 5% CO₂ atmosphere within custom-made microscope stage incubator (CellMovie). Images were acquired every 5 minutes for at least 24 hours using a 10 \times magnification objective. After transfection, the cells were washed 3 times with a serum-containing medium. Time-lapse imaging started one hour after changing the medium. Addition of serum resulted in the flattening of the cells and mitogenic serum factors boosted cell proliferation.

Plasmid transfection experiments. The kinetic treatment of the imaging data addresses the gross kinetics of nuclear dUTPase

accumulation and does not aim to carry out a detailed analysis of the underlying processes. The quantification of fluorescence in single cells from each frame was performed using ImageJ 1.46j (NIH, Bethesda), where the mean nuclear (F_n) and cytoplasmic (F_c) fluorescence were measured. Data points represent mean values extracted from 16 cells in triplicates. The time axis was defined relative to the visual observation of cytokinesis i.e. $t = 0$ at cytokinesis termination. The observed fluorescence intensity increase in the nucleus could be analyzed, as the total fluorescence of the cytoplasmic and nuclear compartments (F_{n+c}) was constant during the time period of the analysis. Single exponential kinetics fit well to the rising phase of the nuclear accumulation curves in both the WT and the S11Q mutant cell lines. The considerable lag in nuclear fluorescence accumulation in the WT cells was not included in the kinetic analysis due to the lack of information on building a comprehensive kinetic model for the whole trafficking process.

Protein transfection experiments. These image sequences were not subjected to densitometric analyses due to lower intensity of the intracellular fluorescent signal as well as to the higher background (Videos S3 and S4). The time elapsed between the onset of cytokinesis and the appearance of fluorescent signal within the nucleus (Fig. S2) was determined by careful visual observation. Considerable nuclear accumulation of fluorescent proteins was declared when the fluorescent intensity within the nucleus exceeded that within the cytoplasm. Parallel phase contrast images were used to determine the onset of cell cleavage.

Both DNA and protein transfection-based experiments yielded the same conclusions regarding the dynamic distribution pattern of the WT and S11Q mutant DsR-DUT. This is potentially due to the fact that the DsRed-labeled proteins can only be detected after a considerable time delay following protein translation, partially because of the time required for maturation of DsRed fluorophore and because of the time required for detectable fluorophore accumulation. Furthermore, newly maturing DsRed molecules (which also went through phosphorylation in M phase) might be in steady state with a degradation process. Because of these effects, the DsR-DUT pool translated during the recording time of video-microscopy used for analysis (~12 hours) does not contribute to the fluorescent signal. The observable fluorescent signal of the mature folded protein molecules thus necessarily originates from the protein pool translated during the cell cycle(s) completed prior to start of the video recording.

Immunoblot analysis

Phosphorylation of the constructs after cellular delivery was investigated using immunoblot analysis. Cells were collected, washed twice with PBS, and resuspended in the lysis buffer (50 mM TRIS-HCl pH = 7.4; 140 mM NaCl; 0.4% NP-40; 2 mM dithiothreitol (DTT); 1 mM EDTA, 1 mM phenylmethylsulfonyl fluoride; 5 mM benzamidin, CompleteTM EDTA free protease inhibitor cocktail tablet (Roche), PhosSTOPTM phosphatase inhibitor cocktail tablet (Roche)). Cell lysis was achieved by sonication. Insoluble fraction was removed by centrifugation (20,000 \times g \times 15 min at 4°C). Protein concentration

was measured with Bio-Rad Protein Assay to ensure equivalent total protein load per lane. Products were resolved under denaturing and reducing conditions on a 15% polyacrylamide gel and transferred to PDVF membrane (Immobilon-P, Millipore). Membranes were blocked with 5% nonfat dried milk, incubated with primary antibodies for 2 hours at room temperature. After washing the membranes secondary antibodies coupled with horseradish peroxidase were applied (Amersham Pharmacia Biotech and Sigma). Immunoreactive bands were visualized by enhanced chemiluminescence reagent (Amersham) and recorded on X-ray film (Kodak). Antibodies to detect the following proteins were used in protein gel blotting: anti-hDUT (1:5000),⁴³ anti-S11P-hDUT (1:200, GenScript).

Recombinant protein production

DsRed-tagged dUTPase constructs were expressed in Rosetta BL21 (DE3) pLysS bacteria strain and purified using Ni-NTA affinity resin (Qiagen). Transformed cells growing in Luria broth medium were induced at $A_{600\text{ nm}}=0.6$ with 0.6 mM isopropyl- β -D-1-thiogalactopyranoside (IPTG) for 16 hours at 20°C. Cells were harvested and lysed in lysis buffer (50 mM TRIS-HCl, pH = 8.0, 300 mM NaCl, 0.5 mM EDTA, 0.1% Triton X-100, 10 mM 2-mercaptoethanol, 1 mM phenylmethylsulfonyl fluoride; 5 mM benzamidin, CompleteTM EDTA free protease inhibitor cocktail tablet (Roche)) with sonication and cell debris was pelleted by centrifugation at 20.000 \times g for 30 minutes. Supernatant was applied onto a Ni-NTA column and washed with lysis buffer containing 50 mM imidazole. dUTPase was finally eluted with elution buffer (50 mM HEPES, pH = 7.5, 30 mM KCl, 500 mM imidazole, 10 mM 2-mercaptoethanol). dUTPase constructs were dialyzed against buffer containing:

20 mM HEPES, pH = 7.4, 140 mM NaCl, 1 mM MgCl₂ and 2 mM dithiothreitol (DTT). The proteins were >95 % pure as assessed by SDS-PAGE.

Disclosure of Potential Conflicts of Interest

No potential conflicts of interest were disclosed.

Acknowledgments

We are grateful to Professor Salvatore Caradonna for providing the UNG2 cDNA.

Funding

This work This work was supported by grants from the by the Hungarian Scientific Research Fund (OTKA NK 84008, OTKA K109486), the Baross program of the New Hungary Development Plan (3DSTRUCT, OMF0-00266/2010 REG-KM-09-1-2009-0050), the Hungarian Academy of Sciences (TTK IF-28/2012), the MedinProt program of the Hungarian Academy of Sciences, and the European Commission FP7 BioStruct-X project (contract No. 283570), to BGV. GR is the recipient of Young Researcher Fellowships from the Hungarian Academy of Sciences. JT is the recipient of the János Bolyai Research Scholarship of the Hungarian Academy of Sciences.

Supplemental Material

Supplemental data for this article can be found on the publisher's website.

References

- Gorlich D, Vogel F, Mills AD, Hartmann E, Laskey RA. Distinct functions for the two importin subunits in nuclear protein import. *Nature* 1995; 377:246-8; PMID:7675110; <http://dx.doi.org/10.1038/377246a0>
- Sorokin AV, Kim ER, Ovchinnikov LP. Nucleocytoplasmic transport of proteins. *Biochem Biokhimiia* 2007; 72:1439-57; PMID:18282135; <http://dx.doi.org/10.1134/S0006297907130032>
- Jans DA. The regulation of protein transport to the nucleus by phosphorylation. *Biochem J* 1995; 311 (Pt 3):705-16; PMID:7487922
- Jans DA, Hubner S. Regulation of protein transport to the nucleus: central role of phosphorylation. *Physiol Rev* 1996; 76:651-85; PMID:8757785
- Nardozi JD, Lott K, Cingolani G. Phosphorylation meets nuclear import: a review. *Cell Commun Signal: CCS* 2010; 8:32; PMID:21182795; <http://dx.doi.org/10.1186/1478-811X-8-32>
- Kosugi S, Hasebe M, Tomita M, Yanagawa H. Systematic identification of cell cycle-dependent yeast nucleocytoplasmic shuttling proteins by yeast identification of composite motifs. *Proc Natl Acad Sci U S A* 2009; 106:10171-6; PMID:19520826; <http://dx.doi.org/10.1073/pnas.0900604106>
- Fontes MR, Teh T, Jans D, Brinkworth RI, Kobe B. Structural basis for the specificity of bipartite nuclear localization sequence binding by importin- α . *J Biol Chem* 2003; 278:27981-7; PMID:12695505; <http://dx.doi.org/10.1074/jbc.M303275200>
- Kobe B, Kampmann T, Forwood JK, Listwan P, Brinkworth RI. Substrate specificity of protein kinases and computational prediction of substrates. *Biochim Biophys Acta* 2005; 1754:200-9; PMID:16172032; <http://dx.doi.org/10.1016/j.bbapap.2005.07.036>
- Zhu G, Liu Y, Shaw S. Protein kinase specificity. A strategic collaboration between kinase peptide specificity and substrate recruitment. *Cell Cycle* 2005; 4:52-6; PMID:15655379; <http://dx.doi.org/10.4161/cc.4.1.1353>
- Holmes JK, Solomon MJ. A predictive scale for evaluating cyclin-dependent kinase substrates. A comparison of p34cdc2 and p33cdk2. *J Biol Chem* 1996; 271:25240-6; PMID:8810285; <http://dx.doi.org/10.1074/jbc.271.41.25240>
- Nigg EA. Cellular substrates of p34(cdc2) and its companion cyclin-dependent kinases. *Trends Cell Biol* 1993; 3:296-301; PMID:14731846; [http://dx.doi.org/10.1016/0962-8924\(93\)90011-O](http://dx.doi.org/10.1016/0962-8924(93)90011-O)
- Songyang Z, Blechner S, Hoagland N, Hoekstra MF, Pwnica-Worms H, Cantley LC. Use of an oriented peptide library to determine the optimal substrates of protein kinases. *Curr Biol: CB* 1994; 4:973-82; PMID:7874496; [http://dx.doi.org/10.1016/S0960-9822\(00\)00221-9](http://dx.doi.org/10.1016/S0960-9822(00)00221-9)
- Ellis JJ, Kobe B. Predicting protein kinase specificity: Predikin update and performance in the DREAM4 challenge. *PLoS One* 2011; 6:e21169; PMID:21829434; <http://dx.doi.org/10.1371/journal.pone.0021169>
- Brinkworth RI, Breil RA, Kobe B. Structural basis and prediction of substrate specificity in protein serine/threonine kinases. *Proc Natl Acad Sci U S A* 2003; 100:74-9; PMID:12502784; <http://dx.doi.org/10.1073/pnas.0134224100>
- Kobe B, Boden M. Computational modelling of linear motif-mediated protein interactions. *Curr Topics Med Chem* 2012; 12:1553-61; PMID:22827524; <http://dx.doi.org/10.2174/156802612802652439>
- Mehdi AM, Sehgal MS, Kobe B, Bailey TL, Boden M. A probabilistic model of nuclear import of proteins. *Bioinformatics* 2011; 27:1239-46; PMID:21372083; <http://dx.doi.org/10.1093/bioinformatics/btr121>
- Saunders NF, Brinkworth RI, Huber T, Kemp BE, Kobe B. Predikin and PredikinDB: a computational framework for the prediction of protein kinase peptide specificity and an associated database of phosphorylation sites. *BMC Bioinformatics* 2008; 9:245; PMID:18501020; <http://dx.doi.org/10.1186/1471-2105-9-245>
- Yaffe MB, Leparo GG, Lai J, Obata T, Volinia S, Cantley LC. A motif-based profile scanning approach for genome-wide prediction of signaling pathways. *Nat Biotechnol* 2001; 19:348-53; <http://dx.doi.org/10.1038/86737>
- Ding R, West RR, Morpheus DM, Oakley BR, McIntosh JR. The spindle pole body of *Schizosaccharomyces pombe* enters and leaves the nuclear envelope as the cell cycle proceeds. *Mol Biol Cell* 1997; 8:1461-79; PMID:9285819; <http://dx.doi.org/10.1091/mbc.8.8.1461>
- Swanson JA, McNeil PL. Nuclear reassembly excludes large macromolecules. *Science* 1987; 238:548-50; PMID:2443981; <http://dx.doi.org/10.1126/science.2443981>
- Vertessy BG, Toth J. Keeping uracil out of DNA: physiological role, structure and catalytic mechanism of dUTPases. *Acc Chem Res* 2009; 42:97-106; PMID:18837522; <http://dx.doi.org/10.1021/ar800114w>
- Rona G, Marfori M, Borsos M, Scheer I, Takacs E, Toth J, Babos F, Magyar A, Erdei A, Bozoky Z,

- et al. Phosphorylation adjacent to the nuclear localization signal of human dUTPase abolishes nuclear import: structural and mechanistic insights. *Acta Crystallogr Section D, Biol Crystallogr* 2013; 69:2495-505; PMID:24311590; <http://dx.doi.org/10.1107/S0907444913023354>
23. Marfori M, Mynott A, Ellis JJ, Mehdi AM, Saunders NF, Curmi PM, Forwood JK, Boden M, Kobe B. Molecular basis for specificity of nuclear import and prediction of nuclear localization. *Biochim Biophys Acta* 2011; 1813:1562-77; PMID:20977914; <http://dx.doi.org/10.1016/j.bbamcr.2010.10.013>
 24. Enserink JM, Kolodner RD. An overview of Cdk1-controlled targets and processes. *Cell division* 2010; 5:11; PMID:20465793; <http://dx.doi.org/10.1186/1747-1028-5-11>
 25. Saunders NF, Kobe B. The Predikin webserver: improved prediction of protein kinase peptide specificity using structural information. *Nucl Acids Res* 2008; 36:W286-90; PMID:18477637; <http://dx.doi.org/10.1093/nar/gkn279>
 26. Geymonat M, Spanos A, Wells GP, Smerdon SJ, Sedgwick SG. Clb6/Cdc28 and Cdc14 regulate phosphorylation status and cellular localization of Swi6. *Mol Cell Biol* 2004; 24:2277-85; PMID:14993267; <http://dx.doi.org/10.1128/MCB.24.6.2277-2285.2004>
 27. Harreman MT, Kline TM, Milford HG, Harben MB, Hodel AE, Corbett AH. Regulation of nuclear import by phosphorylation adjacent to nuclear localization signals. *J Biol Chem* 2004; 279:20613-21; PMID:14998990; <http://dx.doi.org/10.1074/jbc.M401720200>
 28. Sidorova JM, Mikesell GE, Breeden LL. Cell cycle-regulated phosphorylation of Swi6 controls its nuclear localization. *Mol Biol Cell* 1995; 6:1641-58; PMID:8590795; <http://dx.doi.org/10.1091/mbc.6.12.1641>
 29. Kosugi S, Hasebe M, Entani T, Takayama S, Tomita M, Yanagawa H. Design of peptide inhibitors for the importin alpha/beta nuclear import pathway by activity-based profiling. *Chem Biol* 2008; 15:940-9; PMID:18804031; <http://dx.doi.org/10.1016/j.chembiol.2008.07.019>
 30. Dephoure N, Zhou C, Villen J, Beausoleil SA, Bakalarski CE, Elledge SJ, Gygi SP. A quantitative atlas of mitotic phosphorylation. *Proc Natl Acad Sci U S A* 2008; 105:10762-7; PMID:18669648; <http://dx.doi.org/10.1073/pnas.0805139105>
 31. Olsen JV, Vermeulen M, Santamaria A, Kumar C, Miller ML, Jensen LJ, Gnad F, Cox J, Jensen TS, Nigg EA, et al. Quantitative phosphoproteomics reveals widespread full phosphorylation site occupancy during mitosis. *Sci Signal* 2010; 3:ra3; PMID:20068231; <http://dx.doi.org/10.1126/scisignal.2000475>
 32. Stephen AG, Trausch-Azar JS, Handley-Gearhart PM, Ciechanover A, Schwartz AL. Identification of a region within the ubiquitin-activating enzyme required for nuclear targeting and phosphorylation. *J Biol Chem* 1997; 272:10895-903; PMID:9099746; <http://dx.doi.org/10.1074/jbc.272.16.10895>
 33. Lee MK, Tong WM, Wang ZQ, Sabapathy K. Serine 312 phosphorylation is dispensable for wild-type p53 functions in vivo. *Cell Death Differ* 2010; 18:214-21; PMID:20671749; <http://dx.doi.org/10.1038/cdd.2010.90>
 34. Otterlei M, Haug T, Nagelhus TA, Slupphaug G, Lindmo T, Krokan HE. Nuclear and mitochondrial splice forms of human uracil-DNA glycosylase contain a complex nuclear localisation signal and a strong classical mitochondrial localisation signal, respectively. *Nucl Acids Res* 1998; 26:4611-7; PMID:9753728; <http://dx.doi.org/10.1093/nar/26.20.4611>
 35. Fiser A, Vertessy BG. Altered subunit communication in subfamilies of trimeric dUTPases. *Biochem Biophys Res Commun* 2000; 279:534-42; PMID:11118321; <http://dx.doi.org/10.1006/bbrc.2000.3994>
 36. Mustafi D, Bekesi A, Vertessy BG, Makinen MW. Catalytic and structural role of the metal ion in dUTP pyrophosphatase. *Proc Natl Acad Sci U S A* 2003; 100:5670-5; PMID:12721364; <http://dx.doi.org/10.1073/pnas.1031504100>
 37. Vertessy BG, Persson R, Rosengren AM, Zepezauer M, Nyman PO. Specific derivatization of the active site tyrosine in dUTPase perturbs ligand binding to the active site. *Biochem Biophys Res Commun* 1996; 219:294-300; PMID:8604980; <http://dx.doi.org/10.1006/bbrc.1996.0226>
 38. Kovari J, Barabas O, Varga B, Bekesi A, Tolgyesi F, Fidy J, Nagy J, Vertessy BG. Methylene substitution at the alpha-beta bridging position within the phosphate chain of dUDP profoundly perturbs ligand accommodation into the dUTPase active site. *Proteins* 2008; 71:308-19; PMID:17932923; <http://dx.doi.org/10.1002/prot.21757>
 39. Nemeth-Pongracz V, Barabas O, Fuxreiter M, Simon I, Pichova I, Rumlova M, Zabranska H, Svergun D, Petoukhov M, Harmat V, et al. Flexible segments modulate co-folding of dUTPase and nucleocapsid proteins. *Nucl Acids Res* 2007; 35:495-505; PMID:17169987; <http://dx.doi.org/10.1093/nar/gkl1074>
 40. Bekesi A, Zagya I, Hunyadi-Gulyas E, Pongracz V, Kovari J, Nagy AO, Erdei A, Medzihradsky KF, Vertessy BG. Developmental regulation of dUTPase in *Drosophila melanogaster*. *J Biol Chem* 2004; 279:22362-70; PMID:14996835; <http://dx.doi.org/10.1074/jbc.M313647200>
 41. Kovari J, Barabas O, Takacs E, Bekesi A, Dubrovay Z, Pongracz V, Zagya I, Imre T, Szabo P, Vertessy BG. Altered active site flexibility and a structural metal-binding site in eukaryotic dUTPase: kinetic characterization, folding, and crystallographic studies of the homotrimeric *Drosophila* enzyme. *J Biol Chem* 2004; 279:17932-44; PMID:14724274; <http://dx.doi.org/10.1074/jbc.M313643200>
 42. Lari SU, Chen CY, Vertessy BG, Morre J, Bennett SE. Quantitative determination of uracil residues in *Escherichia coli* DNA: Contribution of ung, dug, and dut genes to uracil avoidance. *DNA Repair* 2006; 5:1407-20; PMID:16908222; <http://dx.doi.org/10.1016/j.dnarep.2006.06.009>
 43. Merenyi G, Kovari J, Toth J, Takacs E, Zagya I, Erdei A, Vertessy BG. Cellular response to efficient dUTPase RNAi silencing in stable HeLa cell lines perturbs expression levels of genes involved in thymidylate metabolism. *Nucleosides Nucleotides Nucleic Acids* 2011; 30:369-90; PMID:21780905; <http://dx.doi.org/10.1080/15257770.2011.582849>
 44. Muha V, Horvath A, Bekesi A, Pukancsik M, Hodoscsek B, Merenyi G, Rona G, Batki J, Kiss I, Jankovics F, et al. Uracil-containing DNA in *Drosophila*: stability, stage-specific accumulation, and developmental involvement. *PLoS Genet* 2012; 8:e1002738.
 45. Pecsí I, Hirmondo R, Brown AC, Lopata A, Parish T, Vertessy BG, Toth J. The dUTPase enzyme is essential in *Mycobacterium smegmatis*. *PLoS One* 2012; 7:e37461; PMID:22655049; <http://dx.doi.org/10.1371/journal.pone.0037461>
 46. Ladner RD, Carr SA, Huddleston MJ, McNulty DE, Caradonna SJ. Identification of a consensus cyclin-dependent kinase phosphorylation site unique to the nuclear form of human deoxyuridine triphosphate nucleotidohydrolase. *J Biol Chem* 1996; 271:7752-7; PMID:8631817; <http://dx.doi.org/10.1074/jbc.271.13.7752>
 47. Toth J, Varga B, Kovacs M, Malnasi-Csizmadia A, Vertessy BG. Kinetic mechanism of human dUTPase, an essential nucleotide pyrophosphatase enzyme. *J Biol Chem* 2007; 282:33572-82; PMID:17848562; <http://dx.doi.org/10.1074/jbc.M706230200>
 48. Tinklenberg BA, Fazzone W, Lynch FJ, Ladner RD. Identification of sequence determinants of human nuclear dUTPase isoform localization. *Exp Cell Res* 2003; 287:39-46; PMID:12799180; [http://dx.doi.org/10.1016/S0014-4827\(03\)00048-X](http://dx.doi.org/10.1016/S0014-4827(03)00048-X)
 49. MacFarlane AJ, Anderson DD, Flodby P, Perry CA, Allen RH, Stabler SP, Stover PJ. Nuclear localization of de novo thymidylate biosynthesis pathway is required to prevent uracil accumulation in DNA. *J Biol Chem* 2012; 286:44015-22; <http://dx.doi.org/10.1074/jbc.M111.307629>
 50. Anderson DD, Eom JY, Stover PJ. Competition between sumoylation and ubiquitination of serine hydroxymethyltransferase 1 determines its nuclear localization and its accumulation in the nucleus. *J Biol Chem* 2012; 287:4790-9; PMID:22194612; <http://dx.doi.org/10.1074/jbc.M111.302174>
 51. Woeller CF, Anderson DD, Szebenyi DM, Stover PJ. Evidence for small ubiquitin-like modifier-dependent nuclear import of the thymidylate biosynthesis pathway. *J Biol Chem* 2007; 282:17623-31; PMID:17446168; <http://dx.doi.org/10.1074/jbc.M702526200>
 52. Anderson DD, Woeller CF, Chiang EP, Shane B, Stover PJ. Serine hydroxymethyltransferase anchors de novo thymidylate synthesis pathway to nuclear lamina for DNA synthesis. *J Biol Chem* 2012; 287:7051-62; PMID:22255121; <http://dx.doi.org/10.1074/jbc.M111.333120>
 53. Niida H, Shimada M, Murakami H, Nakanishi M. Mechanisms of dNTP supply that play an essential role in maintaining genome integrity in eukaryotic cells. *Cancer Sci* 2010; 101:2505-9; PMID:20874841; <http://dx.doi.org/10.1111/j.1349-7006.2010.01719.x>
 54. Matsuoka S, Ballif BA, Smogorzewska A, McDonald ER, 3rd, Hurov KE, Luo J, Bakalarski CE, Zhao Z, Solimini N, Lerehthal Y, et al. ATM and ATR substrate analysis reveals extensive protein networks responsive to DNA damage. *Science* 2007; 316:1160-6; PMID:17525332; <http://dx.doi.org/10.1126/science.1140321>
 55. Langerak P, Russell P. Regulatory networks integrating cell cycle control with DNA damage checkpoints and double-strand break repair. *Philos Trans R Soc Lond B Biol Sci* 2012; 366:3562-71; <http://dx.doi.org/10.1098/rstb.2011.0070>
 56. Chakraborty P, Wang Y, Wei JH, van Deursen J, Yu H, Malureanu L, Dasso M, Forbes DJ, Levy DE, Seemann J, et al. Nucleoporin levels regulate cell cycle progression and phase-specific gene expression. *Dev Cell* 2008; 15:657-67; PMID:19000832; <http://dx.doi.org/10.1016/j.devcel.2008.08.020>
 57. Fulcher AJ, Roth DM, Fatima S, Alvisi G, Jans DA. The BRCA-1 binding protein BRAP2 is a novel, negative regulator of nuclear import of viral proteins, dependent on phosphorylation flanking the nuclear localization signal. *FASEB J* 2010; 24:1454-66; PMID:20040518; <http://dx.doi.org/10.1096/fj.09-136564>
 58. Uniprot C. Reorganizing the protein space at the Universal Protein Resource (UniProt). *Nucl Acids Res* 2012; 40:D71-5; PMID:22102590; <http://dx.doi.org/10.1093/nar/gkr981>
 59. Kosugi S, Hasebe M, Matsumura N, Takashima H, Miyamoto-Sato E, Tomita M, Yanagawa H. Six classes of nuclear localization signals specific to different binding grooves of importin alpha. *J Biol Chem* 2009; 284:478-85; PMID:19001369; <http://dx.doi.org/10.1074/jbc.M807017200>
 60. Stark C, Breitkreutz BJ, Reguly T, Boucher L, Breitkreutz A, Tyers M. BioGRID: a general repository for interaction datasets. *Nucl Acids Res* 2006; 34:D535-9; PMID:16381927; <http://dx.doi.org/10.1093/nar/gkj109>
 61. Sorg C, Stamminger T. Mapping of nuclear localization signals by simultaneous fusion to green fluorescent protein and to beta-galactosidase. *Biotechniques* 1999; 26:858-62; PMID:10337476
 62. Gnad F, Gunawardena J, Mann M. PHOSIDA 2011: the posttranslational modification database. *Nucl Acids Res* 2011; 39:D253-60; PMID:21081558; <http://dx.doi.org/10.1093/nar/gkq1159>
 63. Gnad F, Ren S, Cox J, Olsen JV, Macek B, Oroshi M, Mann M. PHOSIDA (phosphorylation site database): management, structural and evolutionary investigation, and prediction of phosphosites. *Genome Biol* 2007; 8:

- R250; PMID:18039369; <http://dx.doi.org/10.1186/gb-2007-8-11-r250>
64. Cimprich KA, Cortez D. ATR: an essential regulator of genome integrity. *Nat Rev Mol Cell Biol* 2008; 9:616-27; PMID:18594563; <http://dx.doi.org/10.1038/nrm2450>
 65. Kim H, Chen J, Yu X. Ubiquitin-binding protein RAP80 mediates BRCA1-dependent DNA damage response. *Science* 2007; 316:1202-5; PMID:17525342; <http://dx.doi.org/10.1126/science.1139621>
 66. Sobhian B, Shao G, Lilli DR, Culhane AC, Moreau LA, Xia B, Livingston DM, Greenberg RA. RAP80 targets BRCA1 to specific ubiquitin structures at DNA damage sites. *Science* 2007; 316:1198-202; PMID:17525341; <http://dx.doi.org/10.1126/science.1139516>
 67. Guerrero-Santoro J, Kapetanaki MG, Hsieh CL, Gorbachinsky I, Levine AS, Rapic-Otrin V. The cullin 4B-based UV-damaged DNA-binding protein ligase binds to UV-damaged chromatin and ubiquitinates histone H2A. *Cancer Res* 2008; 68:5014-22; PMID:18593899; <http://dx.doi.org/10.1158/0008-5472.CAN-07-6162>
 68. Ku WC, Chiu SK, Chen YJ, Huang HH, Wu WG. Complementary quantitative proteomics reveals that transcription factor AP-4 mediates E-box-dependent complex formation for transcriptional repression of HDM2. *Mol Cell Proteomics* 2009; 8:2034-50; PMID:19505873; <http://dx.doi.org/10.1074/mcp.M900013-MCP200>
 69. Jin Q, Yu LR, Wang L, Zhang Z, Kasper LH, Lee JE, Wang C, Brindle PK, Dent SY, Ge K. Distinct roles of GCN5/PCAF-mediated H3K9ac and CBP/p300-mediated H3K18/27ac in nuclear receptor transactivation. *EMBO J* 2011; 30:249-62; PMID:21131905; <http://dx.doi.org/10.1038/emboj.2010.318>
 70. Liu H, Hew HC, Lu ZG, Yamaguchi T, Miki Y, Yoshida K. DNA damage signalling recruits RREB-1 to the p53 tumour suppressor promoter. *Biochem J* 2009; 422:543-51; PMID:19558368; <http://dx.doi.org/10.1042/BJ20090342>
 71. Thiagalingam A, De Bustros A, Borges M, Jasti R, Compton D, Diamond L, Mabry M, Ball DW, Baylin SB, Nelkin BD. RREB-1, a novel zinc finger protein, is involved in the differentiation response to Ras in human medullary thyroid carcinomas. *Mol Cell Biol* 1996; 16:5335-45; PMID:8816445
 72. Iyer NG, Ozdag H, Caldas C. p300/CBP and cancer. *Oncogene* 2004; 23:4225-31; PMID:15156177; <http://dx.doi.org/10.1038/sj.onc.1207118>
 73. Egawa T, Littman DR. Transcription factor AP4 modulates reversible and epigenetic silencing of the Cd4 gene. *Proc Nat Acad Sci U S A* 2011; 108:14873-8; PMID:21873191; <http://dx.doi.org/10.1073/pnas.1112293108>
 74. Imai K, Okamoto T. Transcriptional repression of human immunodeficiency virus type 1 by AP-4. *J Biol Chem* 2006; 281:12495-505; PMID:16540471; <http://dx.doi.org/10.1074/jbc.M511773200>
 75. Guetg C, Lienemann P, Sirri V, Grummt I, Hernandez-Verdun D, Hottiger MO, Fussenegger M, Santoro R. The NoRC complex mediates the heterochromatin formation and stability of silent rRNA genes and centromeric repeats. *EMBO J* 2010; 29:2135-46; PMID:20168299; <http://dx.doi.org/10.1038/emboj.2010.17>
 76. Strohner R, Nemeth A, Jansa P, Hofmann-Rohrer U, Santoro R, Langst G, Grummt I. NoRC—a novel member of mammalian ISWI-containing chromatin remodeling machines. *EMBO J* 2001; 20:4892-900; PMID:11532953; <http://dx.doi.org/10.1093/emboj/20.17.4892>
 77. Jia S, Kobayashi R, Grewal SI. Ubiquitin ligase component Cul4 associates with Clr4 histone methyltransferase to assemble heterochromatin. *Nat Cell Biol* 2005; 7:1007-13; PMID:16127433; <http://dx.doi.org/10.1038/ncb1300>
 78. Blencowe BJ, Bauren G, Eldridge AG, Issner R, Nickerson JA, Rosonina E, Sharp PA. The SRm160/300 splicing coactivator subunits. *RNA* 2000; 6:111-20; PMID:10668804; <http://dx.doi.org/10.1017/S1355838200991982>
 79. Yang L, Li N, Wang C, Yu Y, Yuan L, Zhang M, Cao X. Cyclin L2, a novel RNA polymerase II-associated cyclin, is involved in pre-mRNA splicing and induces apoptosis of human hepatocellular carcinoma cells. *J Biol Chem* 2004; 279:11639-48; PMID:14684736; <http://dx.doi.org/10.1074/jbc.M312895200>
 80. Zou Y, Mi J, Cui J, Lu D, Zhang X, Guo C, Gao G, Liu Q, Chen B, Shao C, et al. Characterization of nuclear localization signal in the N terminus of CUL4B and its essential role in cyclin E degradation and cell cycle progression. *J Biol Chem* 2009; 284:33320-32; PMID:19801544; <http://dx.doi.org/10.1074/jbc.M109.050427>
 81. Miranda-Carboni GA, Krum SA, Yee K, Nava M, Deng QE, Pervin S, Collado-Hidalgo A, Galic Z, Zack JA, Nakayama K, et al. A functional link between Wnt signaling and SKP2-independent p27 turnover in mammary tumors. *Genes Dev* 2008; 22:3121-34; PMID:19056892; <http://dx.doi.org/10.1101/gad.1692808>
 82. Higa LA, Yang X, Zheng J, Banks D, Wu M, Ghosh P, Sun H, Zhang H. Involvement of CUL4 ubiquitin E3 ligases in regulating CDK inhibitors Dacapo/p27Kip1 and cyclin E degradation. *Cell Cycle* 2006; 5:71-7; PMID:16322693; <http://dx.doi.org/10.4161/cc.5.1.2266>
 83. Li HL, Wang TS, Li XY, Li N, Huang DZ, Chen Q, Ba Y. Overexpression of cyclin L2 induces apoptosis and cell-cycle arrest in human lung cancer cells. *Chin Med J (Engl)* 2007; 120:905-9; PMID:17543181
 84. Kondo T, Sheets PL, Zopf DA, Aloor HL, Cummins TR, Chan RJ, Hashino E. Tlx3 exerts context-dependent transcriptional regulation and promotes neuronal differentiation from embryonic stem cells. *Proc Nat Acad Sci U S A* 2008; 105:5780-5; PMID:18391221; <http://dx.doi.org/10.1073/pnas.0708704105>
 85. Worman HJ. Nuclear lamins and laminopathies. *J Pathol* 2011; 226:316-25; PMID:21953297; <http://dx.doi.org/10.1002/path.2999>
 86. Dittmer TA, Misteli T. The lamin protein family. *Genome Biol* 2011; 12:222; PMID:21639948; <http://dx.doi.org/10.1186/gb-2011-12-5-222>